Journal of The Electrochemical Society

OPEN ACCESS

The Poor Academic's DC-Offset for Reversing Polarity in Electrochemical Cells: Application to Redox Flow Cells

Journal of The Electrochemical Society, 2022 **169** 090527

The Poor Academic's DC-Offset for Reversing Polarity in Electrochemical Cells: Application to Redox Flow Cells

Kiana Amini,[*,=] Eric M. Fell,[=,] and Michael J. Aziz[*,z]**

Harvard John A. Paulson School of Engineering and Applied Sciences, 29 Oxford Street, Cambridge, MA, 02138, United States of America

We provide a simple and inexpensive manual DC-offset method for extending the accepted voltage range of a battery cycler to negative voltages, without interfering with the actual operation of the electrochemical cell under the test or exceeding the voltage specs of the battery cycler instrument. We describe the working principles of the method and validate the proposed setup by operating short-term and long-term redox flow battery cycling using compositionally symmetric cell, with open-circuit voltage of zero, and full cell configurations. The method can be used to extend the capability of battery cycler instrumentation to operate any electrochemical cell that requires the polarity to be reversed during operation. Applications include cycling of other symmetric cells (e.g., Li-ion cells), implementation of polarity reversal steps for rejuvenation of electroactive species or rebalancing electrochemical cells, and alternating polarity for electrochemical synthesis.

 [DOI: 10.1149/1945-7111/ac91a8]

Manuscript received August 10, 2022. Published September 22, 2022.

Supplementary material for this article is available online

Renewable sources of energy such as solar and wind are viable options to deliver on the promise of a clean energy future. Nevertheless, the intermittency of these resources can be addressed by the use of a safe and reliable energy storage system.[1] Redox flow batteries (RFBs) are emerging energy storage technologies that are attractive due to their design flexibility, long life, and safety.[2] In RFBs, the redox active species are dissolved in two separate electrolytes and stored externally from the battery stack component. During the charge/discharge, the electrolytes are continuously pumped into the cell, where the electrochemical reactions occur. This modular design decouples the energy and power capacity of the battery, allowing for their independent scale-up and optimization.[3]

To date, a tremendous amount of research has been conducted to develop new electroactive species and characterize their performance in RFBs.[4,5] These cell-level characterizations are commonly conducted in either full cell or symmetric cell configurations.[6,7] In the full cell configuration, two redox reactions of interest are paired, one in the negolyte (negative electrolyte) and another in the posolyte (positive electrolyte) of the battery, and the constructed cell is operated for several days. A full cell RFB is closest to the practical configuration and allows the user to gather information about the charge, voltage, and energy efficiencies of the battery, and the overall capacity fade rate of the system.[8]

A variety of reasons can contribute to the loss of capacity in a battery, including precipitation, crossover, and degradation of either of the negolyte or posolyte electroactive species.[9] To further investigate the isolated contributions of these phenomena, numerous methods have been employed.[10,11] One powerful method is the operation of RFBs in the symmetric cell configuration.[6,12–14] In a symmetric cell, identical redox active molecules with the same compositions are used on both sides of the battery, eliminating crossover as a source of capacity fade in the battery and isolating the characterization to a single redox active molecule. A symmetric cell can be operated with volumetrically unbalanced compositionally-symmetric positive and negative electrolyte reservoirs, which allow for clear identification of a capacity limiting side (CLS) and non-capacity limiting side (NCLS) and permits the attribution of the capacity fade rate to the treatment of the CLS alone.[6] Hence, while a symmetric cell is not a practical battery, it is a powerful method for precise investigation of the degradation of electroactive species in RFBs.

Electrochemical labs focused on battery research are commonly equipped with potentiostats and battery cyclers. While potentiostats can apply voltages over both positive and negative ranges (e.g., ±10 V, or ±15 V) and can be employed for both battery cycling and multi-electrode (e.g., three-electrode) cell setups, battery cyclers are commonly manufactured with only positive voltage capabilities (e.g., 0–5 V, or 0–10 V) and are strictly used for battery cycling. This design of battery cyclers is justified because a battery can be operated with its positive and negative terminals connected to the positive and negative leads of the cycler, respectively, yielding a positive voltage. Additionally, batteries of interest commonly have at least more than hundreds of millivolts of potential difference between their two half cells, allowing a cycler with only positive voltage capabilities to be employed with no issues, even when the battery is discharging into an applied voltage that is hundreds of millivolts smaller than the open circuit voltage. Nevertheless, a battery cycler without negative voltage capabilities cannot be employed for symmetric cell cycling. Because a symmetric cell utilizes the same redox active species on both sides of the battery, a 0 V open circuit voltage (OCV) occurs when both solutions are at the same state of charge (SOC). Thus, a range of negative to positive voltages, depending on the desired applied overpotential, is needed. As a result, research labs equipped with mainly battery cyclers have been incapable or reluctant to conduct symmetric cell analysis for RFBs. In addition, as the field of RFBs has grown, new methods of characterization and operation have been developed which require a wide range of voltage capabilities. For example, it has been shown that the regeneration of anthraquinones can be accomplished with a deep discharge step, wherein a discharge step with negative voltage can be used to regenerate the decomposed compound during battery operation.[15] Having a battery cycler with capabilities of both negative and positive voltages is also useful for applications beyond redox flow batteries. Examples include the operation of symmetric Li-ion cells,[16] rebalancing electrochemical cells by reversing polarity[17] and high-yield electrochemical synthesis by alternating polarity.[18,19] Upgrading the battery cycler equipment to support negative voltage ranges is highly valuable when the user wants to go beyond normal charge/discharge cycling and standard battery configurations.

Extending the capabilities of a battery cycler to negative voltage ranges, if the manufacturing company offers such extension services,

[=]Equal Contribution.
[*]Electrochemical Society Member.
[**]Electrochemical Society Student Member
[z]E-mail: maziz@harvard.edu

is expensive and, depending on the number of channels, can cost many thousands of dollars. Here, we report a simple and significantly less expensive method for extending the range of the voltage operation on a voltage source. In this method, we manually add a DC-offset to the signal sensed by the instrument. This tricks the system into imposing on the battery the user's desired voltage, which may be outside of the battery cycler's voltage range capabilities, while permitting the battery cycler itself to operate within its voltage range. This manual DC-offset can be achieved by a constant voltage source that is incorporated externally from the battery cycler. Any battery chemistry with a relatively flat cell voltage with respect to its state of charge, and a low self-discharge rate, can be used as this constant voltage source.[20,21] In the present work, we use an inexpensive, commercially available nickel-cadmium (NiCd) battery as a constant voltage source. This battery is chosen because it has a long shelf-life and a cell voltage that barely varies with its state of charge until the majority of its capacity is discharged.[22,23] As a result, even in the case of self-discharge at open circuit, the OCV of a NiCd battery does not change significantly. We describe the working principles of this system and validate the setup by conducting short-term and long-term operations with redox flow batteries in both full cell and symmetric cell configurations. This manual DC-offset method allows research labs to extend the capability of their battery cycler instrumentation to operate symmetric bench-scale batteries and employ battery protocols that require negative voltage values. While our focus in the present work is on flow batteries, the manual DC-offset method is not restricted to flow cells and can be employed for other cells or protocols requiring negative voltage ranges (e.g., Li-ion symmetric cell operation[16,24]).

Experimental

Chemicals.—All solutions were prepared using analytical grade reagents and deionized water. Reagents used were potassium ferrocyanide trihydrate, potassium ferricyanide, potassium hydroxide (all purchased from Sigma Aldrich) and 2,6-DPPEAQ (((9,10-dioxo-9,10-dihydroanthracene-2,6-diyl)bis(oxy))bis(propane-3,1-diyl))bis(phosphonic acid) purchased from TCI Chemicals.

Flow battery experiments.—Flow battery experiments were conducted with cell components from Fuel Cell Technologies Inc. (Albuquerque, NM), or in-house cells with PVC end plates. Interdigitated flow fields made up of pyrosealed POCO graphite flow plates were used in each half cell of the battery along with 3 layers of carbon paper (SGL 39AA) per side. Long-term ferro-/ferricyanide symmetric cells used one sheet of woven carbon cloth (AvCarb NCBA 1698) per side. The ferro-/ferricyanide performance in a symmetric cell at pH 14 and its capacity fade due to self-discharge has been extensively studied in a previous work[25] and thus is a well-characterized system for the validation of our setup. The torque applied during cell assembly (for cells from Fuel Cell Technologies Inc.) was 60 lb-in (6.78 N·m) on each of eight 3/8'–24 bolts, thus the load applied per bolt is approximately 800 lbs. For the in-house cells, this torque was 18 1b-in on each of eight 3/8'–24 bolts. All electrodes were baked at 400°C overnight. The geometric area of each electrode was 5 cm^2. The two half cells were separated by either a Nafion 212 or Nafion 117 cation-exchange membrane and a Viton sheet (10 mils) as a gasket. All membranes were soaked in 1 M KOH for over a day before operation. The electrolytes were pumped into the cell using KNF FF12 diaphragm pumps using fluorinated ethylene propylene (FEP) tubing and with a flow rate of 60 ml/min. The cells were operated inside a nitrogen-filled glovebox. For the tests where the positive and negative electrode potentials were monitored, two Hg/HgO reference electrodes (BASi EF-1369) were incorporated in the path of the two electrolytes close to the inlet of each half cell using a custom-made reference electrode holder.[15] The reference electrode holder was composed of two small chambers separated by Nafion 212. One chamber was filled with the supporting electrolyte (1 M KOH) and the other chamber had an inlet and outlet for the flow of the battery electrolyte. The Hg/HgO reference electrode was immersed in the chamber with the supporting electrolyte. The two Hg/HgO reference electrodes showed a potential difference of 72 mV vs an Ag/AgCl reference electrode (271 mV vs SHE) in a solution of 1 M NaOH. The potentials of the positive and negative electrodes of the flow battery and the OCV of the NiCd battery were measured using separate potentiostat channels during operation of the flow battery.

For the manual DC-offset tests, D size 5.0 Ah NiCd batteries (brand name: PKCELL) were purchased from Amazon. The OCV of the purchased NiCd batteries were in the range of 1.2 V—1.3 V. The exact OCV was measured before each experiment. A D-size battery holder with 4 mm banana plugs (brand name: EISCO) was used for holding the NiCd battery and was also purchased from Amazon. The average cost for extending the voltage range of a cycler using a NiCd battery (with a holder) comes out to 16 USD per cycler channel, which research laboratories may find more affordable than purchasing a commercial DC offset.

Cycling tests were conducted by employing the constant current followed by constant voltage (CCCV) protocol. For the short-term cycling tests, a Biologic potentiostat (VSP) with a voltage range of ±10 V was used. For the long-term cycling tests, a Novonix battery cycler with a standard voltage range of 0 to +5 V was employed. A Novonix DC-offset unit was also used for comparison, which provided a shifted voltage range for the battery cycler of –1 to +4 V. In the absence of a manual DC-offset, flow cells with the DPPEAQ | ferrocyanide chemistries were cycled at a constant current of 40 mA cm^{-2}, followed by a constant charging voltage of 1.4 V and discharging voltage of 0.6 V until the current dropped to 1 mA cm^{-2}. Additionally, symmetric flow cells with the ferricyanide/ferrocyanide chemistry were cycled at ±0.2 V by imposing a voltage square wave of amplitude 0.2 V between the terminals. The voltages were modified when a manual DC-offset was incorporated in the battery setup, depending on the number of NiCd batteries used and their respective OCV, as described in the Results section.

Results

Working principles of a manual DC-offset.—In order to understand the working principles of a manual DC-offset, we need to first describe the general operation of a battery cycler. Figure 1a represents a simplified circuit diagram of a battery cycler.[26,27] The setup is capable of maintaining a known potential difference between the working and counter electrodes and records the resulting flow of current. To achieve this, an electronic component called an operational amplifier (op-amp) is employed. An op-amp (Fig. S1a (available online at stacks.iop.org/JES/169/090527/mmedia)) is a three-terminal electronic component with a DC power supply that is capable of amplifying the voltage difference of the inlet terminals.[28] The two inlet terminals are connected across an extremely large impedance, so that negligible current can pass between the inlets, and hence the input voltage signal is fed to the amplifier with negligible ohmic drop. The outlet terminal is connected through a very low impedance and hence current can pass through the outlet terminal. The output voltage is the result of the amplification of the difference between the two input voltage signals. An op-amp can be designed with a feedback loop, in which the output voltage (Fig. S1b) or a portion of the output voltage (Fig. S1c) is fed back to the inlet terminal. This feedback connection between the output of the op-amp and the input terminal forces the difference between the input voltage terminals to be close to zero, meaning that the output voltage of the op-amp adjusts itself to force the two inlet voltages to be nearly identical.

During battery operation, the user sets the desired potential difference ($V_{Desired}$), with reference to the ground. Because $V_{Desired}$ is connected to the inlet of the op-amp, the voltage drop due to ohmic resistance is extremely negligible and hence the desired voltage is fed to the op-amp with high accuracy. The output current

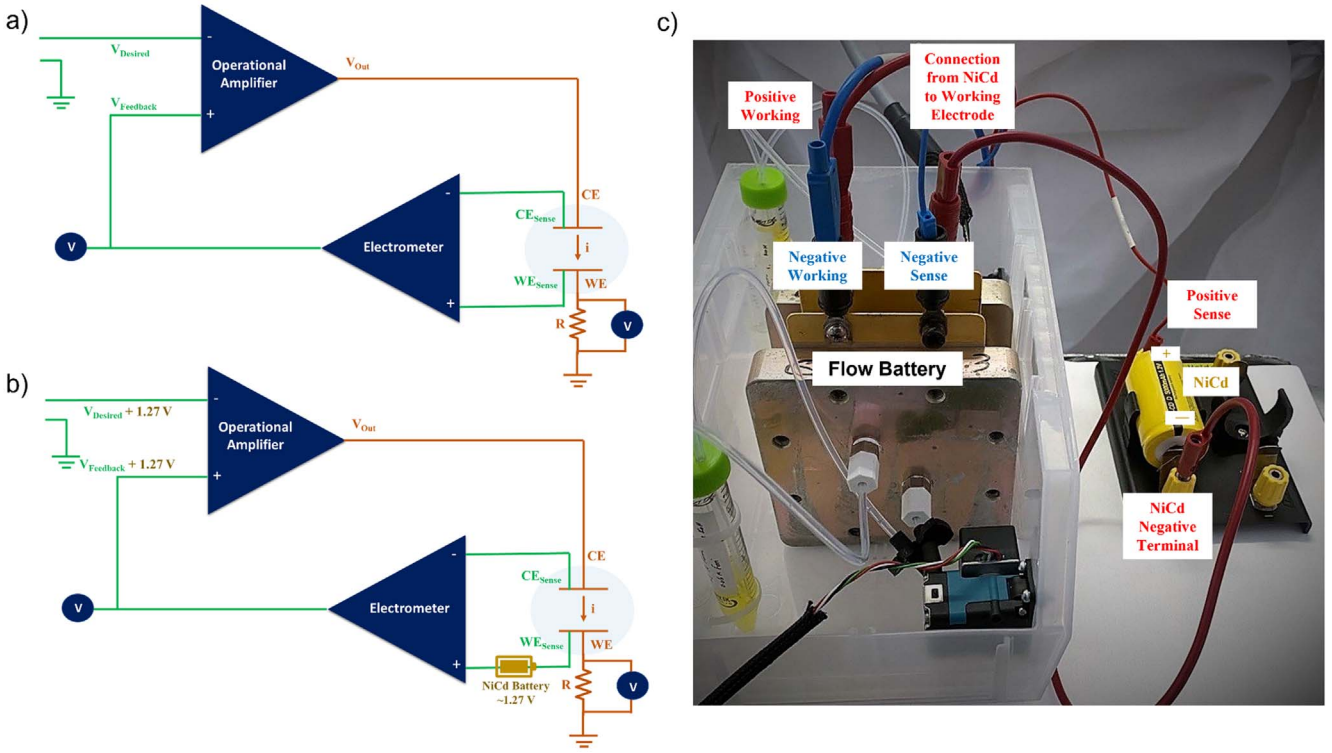

Figure 1. Simplified schematic of a battery cycler (a) without manual DC-offset (adapted from[26] with permission), and (b) with manual DC-offset. (c) Physical implementation of the manual DC-offset in a redox flow battery.

of the op-amp passes between the counter (CE) and working (WE) electrodes of the battery. The counter sense (CE_{Sense}) and the working sense (WE_{Sense}) of the circuit are connected to an electrometer. Note that an electrometer measures the voltage difference between the input signals without drawing current from the circuit due to the extremely large impedance of the electrometer. Thus, current can pass only between the counter and working electrodes and not the sense electrodes. In Figs. 1a and 1b, the paths where negligible current can pass due to extremely large impedance are shown in green, whereas the path of current with low impedance is shown in orange. The flow of current between the counter and working electrodes results in a potential difference between the two electrodes, which is measured and output by the electrometer. The output voltage of the electrometer is connected to the inlet of the op-amp, creating a feedback loop. The op-amp adjusts V_{out} until $V_{Feedback}$ is equal to the user's desired voltage ($V_{Desired}$). Hence, the desired voltage is accurately applied between the counter and working electrodes, and the resulting current is measured by passing it through a resistor (R) connected to the working electrode.

The voltage set by the user must be within the voltage range of the circuit. In order to set negative voltages outside of the cycler's voltage range, a modified circuit diagram shown schematically in Fig. 1b can be employed. In this setup, we simply include one or more NiCd batteries (depending on the amount of offset needed) in the path of either the counter or working sense leads. Here, we have shown the circuit for the case where a single NiCd battery is incorporated in the working sense path. Because the NiCd is incorporated into the WE_{Sense} path, no current will pass through the NiCd battery itself and thus it should remain at its OCV. The WE_{Sense} and CE_{Sense} leads measure the difference between counter and working potentials, identical to the case of Fig. 1a. However, the electrometer will measure the voltage between the two sense leads which now includes the OCV of the NiCd battery. Thus, the feedback voltage will have an additional term corresponding to the OCV of the NiCd battery. To ensure that the difference between the inlet potentials entering the operational amplifier is identical to the case of Fig. 1a with no DC-offset, the value of the OCV of the NiCd must be added to our desired set voltage. With this method, we can successfully apply a desired voltage ($V_{Desired}$) that is outside of the voltage range of the battery cycler, without interfering with the actual operation of the battery being tested or damaging the battery cycler equipment.

In Fig. 1c we show the implementation of the manual DC-offset in practice. On the negative side of the RFB, the CE and CE_{Sense} leads of the battery cycler are connected to the negative terminals of the flow battery, as is standard practice. On the positive side of the RFB, the WE lead of the battery cycler is connected to the positive terminal of the flow battery, similar to the normal operation. However, the WE_{Sense} of the battery cycler is now connected to the positive terminal of a NiCd battery instead of directly connecting to the flow battery. A wire between the negative terminal of the NiCd and positive terminal of the RFB now connects the two batteries in series, as shown in the circuit diagram of Fig. 1b. This configuration allows the user to shift the voltage range of the battery cycler from its standard minimum of 0 V to a new minimum of approximately −1.27 V (negation of the typical OCV for NiCd cells used in this work). Clearly, further negative shifts are possible by using multiple NiCd batteries connected in series.

Half cell electrode potentials in symmetric and full cells with and without manual DC-offset.—For further investigation of the working principles of a manual DC-offset, we monitored the cell voltages as well as positive and negative electrode potentials of an RFB operated with and without a manual DC-offset. This was conducted for both a flow battery operated in the full cell configuration and the symmetric configuration, as is described below.

First, a full cell flow battery composed of 5 ml of 0.1 M DPPEAQ and 50 ml of 0.1 M ferrocyanide/0.04 M ferricyanide at pH 14 was tested. The battery was first operated normally without any manual DC-offset for a cycle. Battery cycling was done using a CCCV method. A current density of 40 mA cm^{-2} was applied

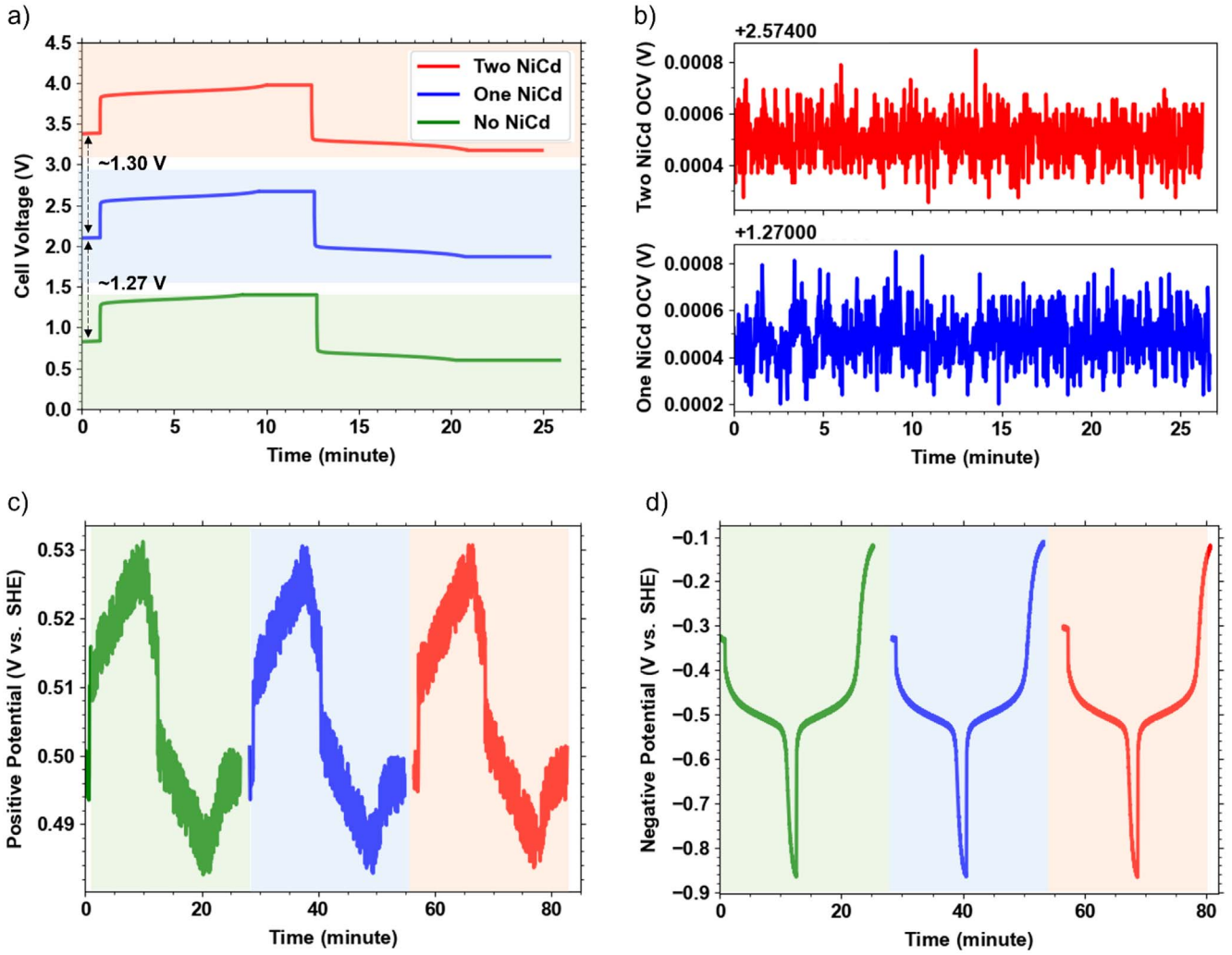

Figure 2. Full cell redox flow battery composed of 5 ml of 0.1 M DPPEAQ and 50 ml of 0.1 M ferro-/0.04 M ferricyanide at pH 14 operated for 3 cycles. The battery is operated with no manual DC-offset, one NiCd, and two NiCds in-series, respectively. A CCCV method with 40 mA cm^{-2} current density and cut-off values of 0.6 − 1.4 V, 1.87 − 2.67 V and 3.17 − 3.97 V were used in the three cycles, respectively. (a) Cell voltage of the redox flow battery during the three described cycles. (b) The OCV of the NiCd batteries monitored during operation. (c) The positive electrode potentials and the (d) negative electrode potentials monitored via in situ reference electrodes during operation.

followed by constant voltages of 1.4 V and 0.6 V until the current dropped to 1 mA cm^{-2}. During the operation, the negative (DPPEAQ) and the positive (ferrocyanide/ferricyanide) electrode potentials were also monitored using the in situ reference electrodes described in the experimental section. Although 0.6 V–1.4 V is within the operational range of the voltage source, we added a manual DC-offset with a NiCd battery to understand the effect of the manual DC-offset method within the same device. The OCV of the incorporated NiCd battery was approximately 1.27 V. As described in the previous section, for correct operation, the OCV of the NiCd battery needs to be added to the user's input voltage values. Hence, the applied voltage cut-off values were changed to 1.87 V and 2.67 V. With no other change, the battery was operated for one cycle. To show the possibility of achieving further voltage shifts, two NiCd batteries connected in series were also incorporated. The two NiCd batteries had OCV values of 1.27 V and 1.30 V, respectively, yielding a total of 2.57 V when connected in series. Hence, the voltage cut-off values were changed to 3.17 V and 3.97 V for the third cycle. The OCV of the NiCd batteries were also monitored during the cycles with DC-offset using a separate potentiostat channel.

The flow cell voltage, negative and positive electrode potentials, and the OCV of the NiCd batteries during operation with the above-described conditions are shown in Fig. 2. As can be seen, the overall cell voltage of the battery is shifted up by ∼1.27 V and ∼2.57 V when one and two NiCd batteries are incorporated in the battery setup, respectively. Nevertheless, the addition of these NiCd batteries has induced virtually no voltage shift in the negative and positive electrode potentials (Figs. 2c and 2d). As discussed previously in relation to Fig. 1b, the addition of a NiCd battery (or multiple NiCd batteries) should not affect the actual potential changes in the positive and negative electrodes. The function of the NiCd batteries is to merely add a constant voltage value to the sensed voltage difference to trick the cycler into accepting the applied/measured voltage. Additionally, because the NiCd batteries are incorporated in the path of the WE_{Sense} lead, no current is passing through them and therefore they always remain at their open circuit voltage. Figure 2b shows the monitored OCV of a single NiCd incorporated during the second cycle and the monitored voltage of the two in-series NiCds incorporated during the third cycle. As can be seen, there were no changes in their voltage during the CCCV operation of the battery.

Next, a flow battery in the symmetric configuration was constructed. It was composed of 0.1 M ferro–/0.1 M ferricyanide in 1 M KOH, with a 4 ml CLS and a 50 ml NCLS. The battery was operated using a potentiostat capable of applying negative voltage

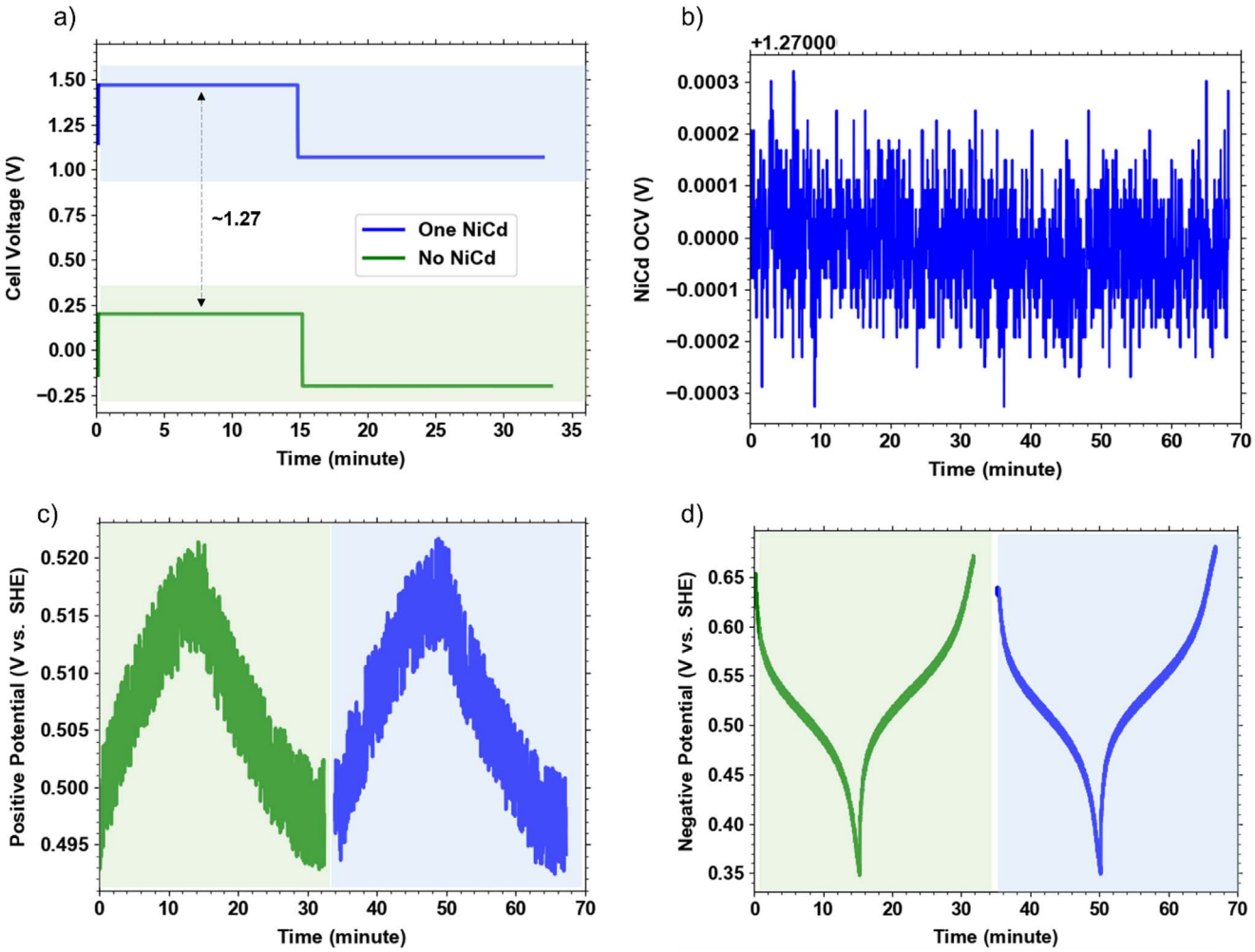

Figure 3. Symmetric redox flow battery composed of 0.1 M ferro-/0.1 M ferricyanide in 1 M KOH (4 ml CLS vs 50 ml NCLS) operated for 2 cycles. The battery is operated with no manual DC-offset and one incorporated NiCd, respectively. A constant charging/discharging voltage of ±0.2 V in the first cycle (no manual DC-offset) and +1.07 V / +1.47 V in the second cycle (with manual DC-offset) was used. (a) Cell voltage of the redox flow battery during the three described cycles. (b) The voltage of the NiCd battery monitored during operation with manual DC-offset. (c) The positive electrode potentials and the (d) negative electrode potentials monitored via in situ reference electrodes during operation.

values (±15 V) to be able to directly investigate the effect of the manual DC-offset in one device. The symmetric cell was first cycled with constant charging and discharging voltages of ±0.2 V until the current drops to 1 mA cm^{-2} (constant voltage method). Next, a single NiCd battery with an OCV of ∼1.27 V was incorporated in the battery setup. Hence, the operational condition in the second cycle was changed to +1.07 V and +1.47 V. Similar to the full cell configuration, the addition of the manual DC-offset affected only the overall measured cell voltage of the symmetric battery (Fig. 3a), with no changes induced in the negative and positive electrode potentials (Figs. 3c and 3d). Additionally, the NiCd battery always remains at its OCV during the operation as shown in Fig. 3b. As can be seen, to run a symmetric cell, we need a voltage source that is capable of applying both negative and positive voltages (±0.2 V), however with this simple manual DC-offset, we are able to run the symmetric cell using a voltage source (such as a battery cycler) that is capable of applying only positive voltage values (+1.07 V and +1.47 V) without any interference to the flow battery operation.

Long-term operation of redox flow batteries with manual DC-Offset.—To investigate the possibility of employing the manual DC-offset method during prolonged operation of redox flow batteries, long-term cycling of a flow battery in full cell configuration and symmetric cell configuration, with and without manual DC-offset, was conducted.

First, a full cell composed of 5 ml 0.1 M DPPEAQ in the negolyte and 50 ml 0.1 M ferro–/0.04 M ferricyanide at pH 14 was constructed. The battery was operated for more than 4 d using the CCCV method. At each cycle a constant current of 40 mA cm^{-2} and voltage cut-off values of 0.6 V and 1.4 V, in the absence of a manual DC-offset, were applied until the current density dropped to 1 mA cm^{-2}. After 4.5 d, the battery was stopped and a single NiCd battery (OCV ∼1.27 V) was incorporated in the setup in the manner described previously. The cut-off values were changed to 1.87 V and 2.67 V (Fig. S2), and the battery was operated for another ∼ 4.5 d. As shown in Fig. 4, the incorporation of the manual DC-offset has had no effect on the measured coulombic efficiency (∼100% in both cases) or the capacity fade rate of the battery (∼0.06%/day in both cases) over several days of operation, demonstrating that the incorporated NiCd has not affected the operation of the flow battery. We tentatively attribute the jump in discharge capacity upon adding the DC offset to the moving of the cell and reservoirs, which might have shaken loose a droplet of electrolyte clinging to the reservoir wall in the head space. When users do not have access to a cycler capable of applying negative voltages, a full cell battery, such as the one put together in the

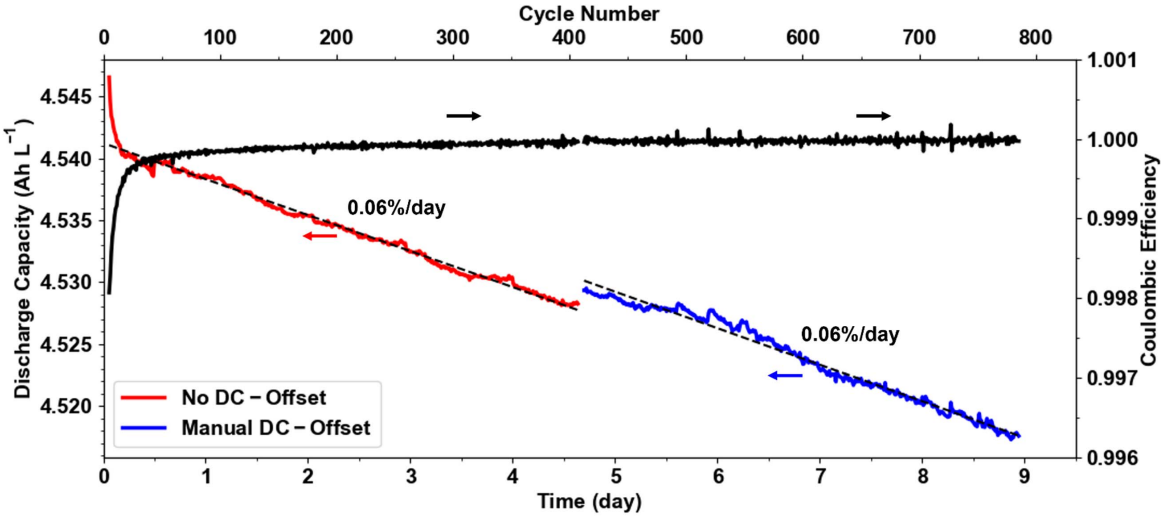

Figure 4. Extended cell cycling performance of 5 ml 0.1 M DPPEAQ at pH 14 paired with 50 ml of 0.1 M ferro-/0.04 M ferricyanide at pH 14. Discharge capacities and coulombic efficiencies vs time and cycle number for a cell, with and without a manual DC-offset.

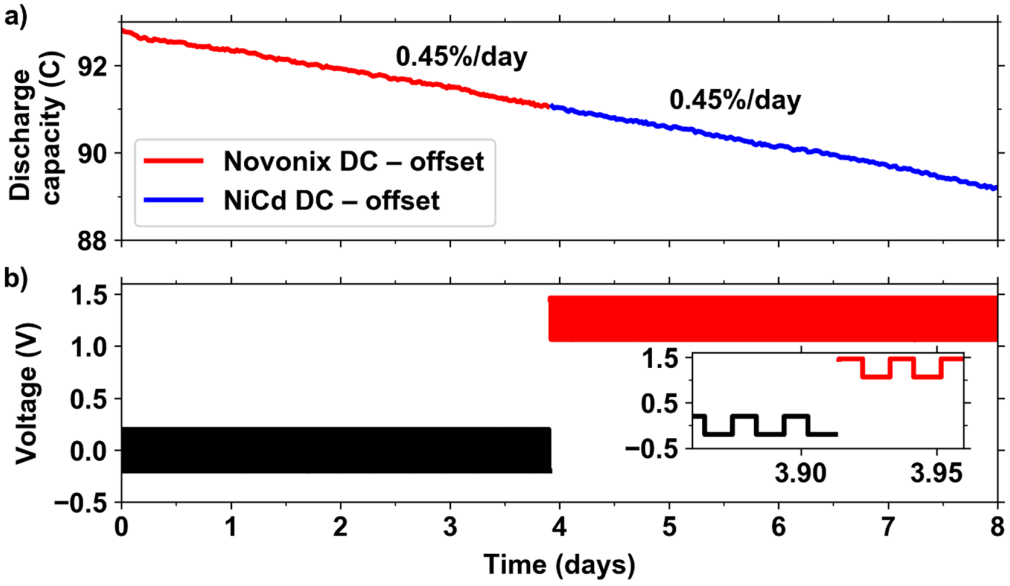

Figure 5. (a) Long-term potentiostatic cycling of a 0.1 M ferro-/0.1 M ferricyanide pH 14 symmetric cell (5 ml CLS vs 10 ml NCLS). After ∼4 d of charge/discharge cycling at ±0.2 V with a Novonix DC-offset (black), a NiCd DC-offset (+1.26 V) was then used with the Novonix in battery cycler mode (red). (b) cell voltage and inset of zoomed in voltage profiles near day 4 when DC-offsets were switched.

present work, can be used for validation of their setup before using the setup for symmetric cell cycling or for an operation that requires application of negative voltages.

As a final demonstration of the DC-offset method, we employed the technique in the long-term operation of a symmetric cell RFB, in which negative voltages are required for cell cycling. A 0.1 M ferro-/0.1 M ferricyanide symmetric cell at pH 14 (5 ml CLS vs 10 ml NCLS) was cycled potentiostatically at ±0.2 V on a Novonix channel equipped with a DC-offset, as seen in Fig. 6. After approximately four days, cycling was paused, the Novonix DC-offset was replaced by a NiCd DC-offset (as described in previous sections) and cycling was continued. The OCV of the NiCd on its own was first measured to be ∼1.27 V, thus when connected in series with the symmetric RFB, charge/discharge cycling was performed at 1.07 V/1.47 V to mimic the desired ±0.2 V cycling protocol typically employed. We observed no change in the capacity fade trend upon switching to our manual NiCd DC-offset (Fig. 5a), demonstrating that the incorporated NiCd offset has not affected the operation of the flow battery.

As explained previously, the NiCd battery remains at its open-circuit potential at all times during the experiment. The stability of the OCV of the NiCd battery during the course of the experiment is essential for achieving an accurate offset. Hence, we monitored the change in the OCV of a NiCd battery over the course of two months by storing a NiCd battery in a glovebox and measuring its OCV periodically, as seen in Fig. 6a. During that time, the NiCd demonstrated an overall self-discharge rate of roughly 12 μV per day over the span of two months. However, OCV measurements at approximately day 21 and 42 show a significant departure from the self-discharge trend. As seen in Fig. 6b, the temperature within the glovebox typically oscillated between 20 and 22 °C, due to diurnal temperature swings within the lab. However, temperature spikes coinciding with the OCV measurement outliers were observed, due to elevated temperature cycling of RFBs being conducted in a separate

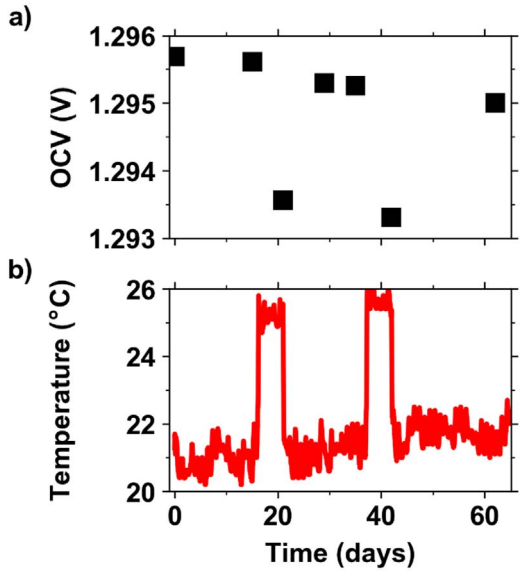

Figure 6. Shelf life of a NiCd battery. (a) OCV measured sporadically the span of two months in a glovebox. (b) recorded temperature of the glovebox over the same period. Temperature spikes occurring at approximately 17 and 37 d correspond to elevated temperature cycling of separate RFBs within the same glovebox.

experiment within the same glovebox. The separate experiments provided unintended data regarding the effect of temperature on the NiCd OCV, which decreased by approximately 2 mV for a 4 °C increase in glovebox temperature. Therefore, it is clearly demonstrated that, if temperature excursions are minimized, NiCd batteries can be used as DC-offsets for multiple weeks before any adjustment of the applied voltage for cycling needs be made, if required to counteract the OCV change. Alternatively, for experiments expanded over many months, the NiCd battery could be replaced or Li-ion batteries with significantly lower self-discharge rates could be employed. No matter the chosen battery chemistry for use as DC-offset, the outlined method provides an extremely cost-effective alternative to cycler manufacturer upgrades, and rapidly extends the capabilities of battery cyclers.

Conclusions

In the present work, we introduced a simple and inexpensive method to manually extend the voltage range of a battery cycler. In this method, a nickel-cadmium battery is incorporated in the path of the battery cycler's voltage sense, tricking the instrument into accepting the user's desired applied voltage, while permitting the battery cycler itself to operate within its voltage range. The working principles of this proposed manual DC-offset are described and validated by operation of flow batteries with and without the proposed manual voltage offset and by monitoring half cell potentials using in situ reference electrodes. The method is further validated by conducting long-term symmetric and full cell cycling experiments. The proposed manual DC-offset method is an inexpensive technique for extending the capability of the battery cycler instrumentation to operate symmetric flow batteries and employ battery protocols that require negative voltage values. The method is not restricted to flow cells and can be employed for extending the voltage range of a cycler for operation of other electrochemical cells.

Acknowledgments

K.A. was supported in part by U.S. DOE award DE-AC05–76RL01830 through PNNL subcontract 535264 and in part through the Natural Sciences and Engineering Research Council of Canada (NSERC) Postdoctoral Fellowship (PDF) program [application number PDF – 557232–2021]. EMF was supported by the National Science Foundation through grant CBET-1914543.

ORCID

Kiana Amini https://orcid.org/0000-0003-2749-7048
Eric M. Fell https://orcid.org/0000-0003-2046-1480
Michael J. Aziz https://orcid.org/0000-0001-9657-9456

References

1. M. Y. Suberu, M. W. Mustafa, and N. Bashir, "Energy storage systems for renewable energy power sector integration and mitigation of intermittency." *Renew. Sustain. Energy Rev.*, **35**, 499 (2014).
2. A. Z. Weber, M. M. Mench, J. P. Meyers, P. N. Ross, J. T. Gostick, and Q. Liu, "Redox flow batteries: a review." *J. Appl. Electrochem.*, **41**, 1137 (2011).
3. B. R. Chalamala, T. Soundappan, G. R. Fisher, M. R. Anstey, V. V. Viswanathan, and M. L. Perry, "Redox flow batteries: an engineering perspective." *Proc. IEEE*, **102**, 976 (2014).
4. D. G. Kwabi, Y. Ji, and M. J. Aziz, "Electrolyte lifetime in aqueous organic redox flow batteries: a critical review." *Chem. Rev.*, **120**, 6467 (2020).
5. J. Noack, N. Roznyatovskaya, T. Herr, and P. Fischer, "The chemistry of redox-flow batteries." *Angew. Chem. Int. Ed.*, **54**, 9776 (2015).
6. M.-A. Goulet and M. J. Aziz, "Flow battery molecular reactant stability determined by symmetric cell cycling methods." *J. Electrochem. Soc.*, **165**, A1466 (2018).
7. Y. A. Gandomi, D. Aaron, J. Houser, M. Daugherty, J. Clement, A. Pezeshki, T. Ertugrul, D. Moseley, and M. Mench, "Critical review—experimental diagnostics and material characterization techniques used on redox flow batteries." *J. Electrochem. Soc.*, **165**, A970 (2018).
8. K. Amini and M. D. Pritzker, "Life-cycle analysis of Zinc-Cerium redox flow batteries." *Electrochim. Acta*, **356**, 136785 (2020).
9. Q. Chen, L. Eisenach, and M. J. Aziz, "Cycling analysis of a quinone-bromide redox flow battery." *J. Electrochem. Soc.*, **163**, A5057 (2016).
10. O. Nolte, I. A. Volodin, C. Stolze, M. D. Hager, and U. S. Schubert, "Trust is good, control is better: a review on monitoring and characterization techniques for flow battery electrolytes." *Materials Horizons*, **8**, 1866 (2021).
11. Y. Yao, J. Lei, Y. Shi, F. Ai, and Y.-C. Lu, "Assessment methods and performance metrics for redox flow batteries." *Nat. Energy*, **6**, 582 (2021).
12. R. M. Darling and M. L. Perry, "Half-cell, steady-state flow-battery experiments." *ECS Trans.*, **53**, 31 (2013).
13. J. D. Milshtein, J. L. Barton, R. M. Darling, and F. R. Brushett, "4-Acetamido-2, 2, 6, 6-Tetramethylpiperidine-1-Oxyl as a model organic redox active compound for nonaqueous flow batteries." *J. Power Sources*, **327**, 151 (2016).
14. J. D. Milshtein, A. P. Kaur, M. D. Casselman, J. A. Kowalski, S. Modekrutti, P. L. Zhang, N. H. Attanayake, C. F. Elliott, S. R. Parkin, and C. Risko, "High current density, long duration cycling of soluble organic active species for non-aqueous redox flow batteries." *Energy Environ. Sci.*, **9**, 3531 (2016).
15. Y. Jing, E. W. Zhao, M.-A. Goulet, M. Bahari, E. M. Fell, S. Jin, A. Davoodi, E. Jónsson, M. Wu, and C. P. Grey, "In Situ electrochemical recomposition of decomposed redox-active species in aqueous organic flow batteries." *Nat. Chem.*, **1** (2022).
16. J. Burns, L. Krause, D.-B. Le, L. Jensen, A. Smith, D. Xiong, and J. Dahn, "Introducing Symmetric Li-Ion cells as a tool to study cell degradation mechanisms." *J. Electrochem. Soc.*, **158**, A1417 (2011).
17. S. Jin, M. Wu, Y. Jing, R. G. Gordon, and M. J. Aziz, "Low energy carbon capture via electrochemically induced Ph swing with electrochemical rebalancing." *Nat. Commun.*, **13**, 1 (2022).
18. Y. Kawamata, K. Hayashi, E. Carlson, S. Shaji, D. Waldmann, B. J. Simmons, J. T. Edwards, C. W. Zapf, M. Saito, and P. S. Baran, "Chemoselective electrosynthesis using rapid alternating polarity." *JACS*, **143**, 16580 (2021).
19. C. Schotten, C. J. Taylor, R. A. Bourne, T. W. Chamberlain, B. N. Nguyen, N. Kapur, and C. E. Willans, "Alternating polarity for enhanced electrochemical synthesis." *Reaction Chemistry & Engineering*, **6**, 147 (2021).
20. S. D. Grigorescu, C. Cepisca, and V. Cimpoeru, "Virtual instrumentation based laboratory for batteries testing." *presented at the 2013 8TH International Symposium On Advanced Topics In Electrical Engineering (ATEE), 2013 (unpublished)*.
21. G. Ablay, "Online condition monitoring of battery systems with a nonlinear estimator." *IEEE Trans. Energy Convers.*, **29**, 232 (2013).
22. W. R. Scott and D. W. Rusta, "Sealed-cell nickel-cadmium battery applications manual." (1979).
23. N. Kularatna, "Rechargeable batteries and their management." *IEEE Instrumentation & Measurement Magazine*, **14**, 20 (2011).
24. C. Shen, D. Xiong, L. Ellis, K. L. Gering, L. Huang, and J. Dahn, "Using the charge-discharge cycling of positive electrode symmetric cells to find electrolyte/electrode combinations with minimum reactivity." *J. Electrochem. Soc.*, **164**, A3349 (2017).
25. E. M. Fell, D. De Porcellinis, Y. Jing, V. Gutierrez-Venegas, R. G. Gordon, S. Granados-Focil, and M. J. Aziz, "Long-term stability of ferri-/ferrocyanide as an electroactive component for redox flow battery applications: on the origin of apparent capacity fade." (2022), ChemRxiv.
26. Pine Research, What Is a Potentiostat and How Does It Work?, accessed June 2022, https://pineresearch.com/shop/kb/theory/instrumentation/what-potentiostat-does/.
27. A. W. Colburn, K. J. Levey, D. O'Hare, and J. V. Macpherson, "Lifting the lid on the potentiostat: a beginner's guide to understanding electrochemical circuitry and practical operation." *Phys. Chem. Chem. Phys.*, **23**, 8100 (2021).
28. W. Jung, *Op Amp Applications Handbook.* (Newnes) (2005).